Environmental Science & Technology

Article

pubs.acs.org/est

Thermodynamic Controls on the Microbial Reduction of Iron-Bearing Nontronite and Uranium

Fubo Luan, Christopher A. Gorski, and William D. Burgos*

Department of Civil and Environmental Engineering, The Pennsylvania State University, University Park, Pennsylvania 16802-1408, United States

Supporting Information

ABSTRACT: Iron-bearing phyllosilicate minerals help establish the hydrogeological and geochemical conditions of redox transition zones because of their small size, limited hydraulic conductivity, and redox buffering capacity. The bioreduction of soluble U(VI) to sparingly soluble U(IV) can promote the reduction of clay-Fe(III) through valence cycling. The reductive precipitation of U(VI) to uraninite was previously reported to occur only after a substantial percentage of clay-Fe(III) had been reduced. Using improved analytical techniques, we show that concomitant bioreduction of both U(VI) and clay-Fe(III) by *Shewanella putrefaciens* CN32 can occur. Soluble electron shuttles were previously shown to enhance both the rate and extent of clay-Fe(III) bioreduction. Using extended incubation periods, we show that electron shuttles enhance only the rate of reduction (overcoming a kinetic limitation) and not the final extent of reduction (a thermodynamic limitation). The first 20% of clay-Fe(III) in nontronite NAu-2 was relatively "easy" (i.e., rapid) to bioreduce; the next 15% of clay-Fe(III) was "harder" (i.e., kinetically limited) to bioreduce, and the remaining 65% of clay-Fe(III) was effectively biologically unreducible. In abiotic experiments with NAu-2 and biogenic uraninite, 16.4% of clay-Fe(III) was reduced in the presence of excess uraninite. In abiotic experiments with NAu-2 and reduced anthraquinone 2,6-disulfonate (AH_2DS), 18.5−19.1% of clay-Fe(III) was reduced in the presence of excess and variable concentrations of AH_2DS. A thermodynamic model based on published values of the nonstandard state reduction potentials at pH 7.0 (E'_H) showed that the abiotic reactions between NAu-2 and uraninite had reached an apparent equilibrium. This model also showed that the abiotic reactions between NAu-2 and AH_2DS had reached an apparent equilibrium. The final extent of clay-Fe(III) reduction correlated well with the standard state reduction potential at pH 7.0 ($E^{o\prime}_H$) of all of the reductants used in these experiments (AH_2DS, CN32, dithionite, and uraninite).

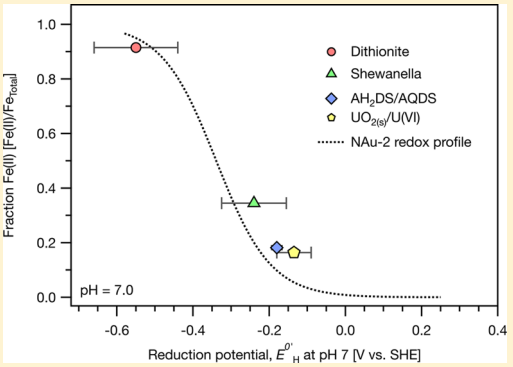

INTRODUCTION

Iron-bearing clay minerals are ubiquitous in soil and sediments and are thought to be the most abundant Fe-containing phase in the Earth's crust,[1] where they can participate in a variety of redox reactions. Structural ferric iron [Fe(III)] in Fe-bearing clay minerals may be reduced by dissimilatory metal reducing bacteria,[2] and structural ferrous iron [Fe(II)] may reduce a wide range of environmental contaminants, such as metals,[3] organic compounds,[4,5] and radionuclides,[6] altering their toxicity and mobility. Of particular interest is the reduction of soluble, oxidized uranyl [U(VI)] to insoluble, reduced uraninite [U(IV)] by structural Fe(II) in clay minerals because of the large number of U.S. Department of Energy (DOE) sites that are contaminated with U and findings that at many of these sites, the majority of Fe is present as a structural component of clay minerals.[7,8] The most favorable approach to remediating U-contaminated sites in a cost-effective manner that has been proposed[9] and tested[10,11] is to stimulate biological Fe-reducing bacteria through the addition of an electron donor. Fe-reducing bacteria can directly respire on U(VI) or can produce Fe(II) that can indirectly reduce U(VI), where both processes produce sparingly soluble uraninite [$U(IV)O_2(s)$].

Despite extensive work, it remains unclear what parameters control the kinetics and extent of U reduction and what parameters control clay mineral-Fe(III) reduction in these systems. Several factors have been hypothesized to explain the rates and extent of structural Fe reduction, including the microorganism and mineral used, the presence or absence of an electron shuttle, and the solution chemistry.[12] Elucidating general trends among studies to isolate the effects of each of these variables is challenging because of reported inconsistencies. For example, some studies have reported that the presence of electron shuttles, such as anthraquinone 2,6-disulfonate (AQDS), increases the extent of structural Fe(III) reduction in clay minerals,[13−15] while other studies have argued that AQDS

Received: November 4, 2013
Revised: February 4, 2014
Accepted: February 10, 2014
Published: February 10, 2014

   dx.doi.org/10.1021/es404885e | Environ. Sci. Technol. 2014, 48, 2750−2758

Table 1. Summary of Reduction Rates and Extents of Nontronite NAu-2 and Reduction Rates of U(VI) under Varied Experimental Conditions

		experimental components					reduction rate		
	reaction description	CN32	NAu-2 or Al_2O_3 (g/L)	U(VI) (μM)	AQDS/AH_2DS (μM)	lactate (mM)	time (h)	k (μM/h)	extent of NAu-2 reduction (%)
Figure 1	bioreduction of NAu-2	1×10^8	2.0	0	0	5	0–41	10.7 Fe	22.2
							41–168	10.0 Fe	
							168–240	1.47 Fe	
Figure 1	bioreduction of U(VI)	1×10^8	0	830	0	5	0–41	17.6 U	–
							41–168	0.17 U	
							168–240	0.01 U	
Figure 1	bioreduction of NAu-2 and U(VI)	1×10^8	2.0	830	0	5	0–41	40.3 Fe/ 9.49 U	22.5
							41–168	1.28 Fe/ 2.45 U	
							168–240	0.45 Fe/ 0.14 U	
Figure S1	bioreduction of U(VI) in the presence of Al_2O_3	1×10^8	2.0 Al_2O_3	830	0	5	0–41	15.7 U	–
							41–168	0.61 U	
							168–240	0.08 U	
Figure 2	bioreduction of NAu-2	1×10^8	2.0	0	0	15	0–96	20.1 Fe	34.5
							168–900	1.11 Fe	
Figure 2	bioreduction of NAu-2 and AQDS	1×10^8	2.0	0	100	15	0–96	27.7 Fe	35.9
							96–900	0.35 Fe	
Figure 4	abiotic reduction of NAu-2 by AH_2DS	0	0.25	0	200–800	0	0–48	3.80 Fe	18.0–19.0
Figure 4	abiotic reduction of NAu-2 by AH_2DS	0	1.0	0	400–800	0	0–27	27.1 Fe	17.4–18.2
Figure 5	abiotic reduction of NAu-2 by biogenic uraninite	0	2.0	0	0	0	0–240	1.76 Fe	8.8
								0.97 U	
not displayed	abiotic reduction of NAu-2 by biogenic uraninite	0	0.5	0	0	0	0–192	1.26 Fe/ 0.59 U	16.4
							192–2016	0.05 Fe/ 0.02 U	
Figure S6	abiotic reduction of NAu-2 by sodium dithionite	0	2.0	0	0	0	0–456	16.4 Fe	91.5

simply enhances only the reduction rate, and not the extent.[16] However, there is no satisfactory explanation at this time.

Additionally, how bacteria, clay minerals, and contaminants interact with one another during bioreduction experiments is largely unknown. Many studies examining contaminant reduction by structural Fe(II) in clay minerals use chemically reduced specimens, which may significantly differ from those produced by biological reduction.[5,17,18] In studies using bioreduced clay minerals, the experiments were often conducted in a two-stage manner in which Fe-bearing clay minerals were first exposed to Fe(III)-reducing bacteria and then subsequently spiked with U or another contaminant.[19] A weakness with this approach is that it does not account for the role that U or another contaminant may play in the bioreduction process. Specifically, it is unclear from these studies if U plays an active or passive role in the bioreduction of structural Fe in clay minerals.

To address these questions, we examined the co-reduction of structural Fe(III) in the Fe-rich nontronite NAu-2 and U(VI) by *Shewenalla putrefaciens* CN32. In our first experiments, we examined if U played an active or passive role in the bioreduction of structural Fe(III) by tracking the rate and extent of reduction. We hypothesized that U would play an active role by serving as an electron shuttle for the bacteria, which would influence the kinetics, but not the extent, of reduction. Experiments were also conducted to determine what factors influence the extent of reduction, including the presence or absence of an electron shuttle and the length of the incubation period. We also performed a series of abiotic experiments in which NAu-2 was exposed to biogenic uraninite [U(IV)], reduced AQDS (AH_2DS), or dithionite. Using reduction potential values for NAu-2 recently measured by our group,[20] we found good agreement between calculated reduction potential values of structural Fe(II)/Fe(III) in NAu-2, U(IV)/U(VI), and AQDS/AH_2DS, suggesting that thermodynamics likely controls the extent of bioreduction of clay minerals in natural systems.

MATERIALS AND METHODS

Microorganism Preparation. *S. putrefaciens* CN32 was grown aerobically on tryptic soy broth without dextrose (Difco) at 20 °C. Cells were harvested and prepared anaerobically as previously described.[21]

Clay Mineral Preparation. Nontronite NAu-2 was purchased from the source clays repository of the Clay Minerals Society (West Lafayette, IN). Keeling et al.[22] have reported the solid-phase mineral composition of NAu-2 to be $M^+_{0.72}(Si_{7.55}Al_{0.16}Fe_{0.29})(Al_{0.34}Fe_{3.54}Mg_{0.05})O_{20}(OH)_4$, where M

dx.doi.org/10.1021/es404885e | Environ. Sci. Technol. 2014, 48, 2750–2758

can be Ca, Na, or K. NAu-2 was suspended in 0.5 M NaCl for 24 h and then separated by centrifugation, yielding the 0.5−2.0 μm clay size fraction. The clay fraction was washed with distilled deionized water (Milli-Q) repeatedly until no Cl^- was detected by silver nitrate and then dried at 60 °C. The NAu-2 clay fraction contained 4.1 mmol of Fe/g of clay, and 99.4% was Fe(III) based on anoxic HF-H_2SO_4/phenanthroline digestion.[23] A NAu-2 clay fraction stock solution (20 g/L) was prepared in deoxygenated 30 mM $NaHCO_3$ buffer (pH 7.0).

Bioreduction of Unaltered Nontronite. All experiments were conducted in 20 mL serum bottles crimp-sealed with rubber stoppers. All preparations were performed in an anoxic chamber (Coy, Grass Lakes, MI) supplied with a 95:5 N_2/H_2 atmosphere. The anoxic chamber was in a 20 °C constant-temperature room. Reactors were filled with ∼15 mL of deoxygenated 10 mM PIPES/30 mM $NaHCO_3$ buffer (pH 7.0; hereafter termed PB buffer) containing various combinations of CN32 (1×10^8 cells/mL), NAu-2 (2.0 g/L), uranyl acetate [U(VI), 830 μM], and AQDS (100 μM). Sodium lactate (5 mM) was provided as the electron donor unless otherwise stated. A series of control reactors in the absence of CN32, NAu-2, or U(VI) were prepared with every experiment. Al_2O_3 (2.0 g/L) was used as a redox-inactive mineral control. All treatments and controls were prepared in triplicate. Reactors were incubated at 100 rpm on orbital shakers within the anoxic chamber. After cell inoculation, samples were periodically removed with sterile needles and syringes. Samples were analyzed for a suite of operationally defined Fe(II) and U(VI) concentrations described below. All sampling and chemical analyses were performed in the anoxic chamber.

Bioreduction of Partially Reduced Nontronite. A series of experiments were initiated after the nontronite and U(VI) had been bioreduced by CN32 for 240 h, or nontronite alone [i.e., no U(VI)] had been bioreduced by CN32 for 340 h. These incubation periods were selected because the extents of bioreduction of clay-Fe(III) were nearly complete under our reaction conditions. After these so-called "preliminary manipulations" were completed, the reactor systems were reinoculated with CN32 and lactate or with CN32 and lactate and U(VI) (Table 1). These experiments were designed to better define the final extent of clay-Fe(III) and U(VI) reduction and to study a scenario in which U(VI) enters already-reduced subsurface sediments.

Experimental procedures were identical to those described above. For the preliminary manipulation used to examine the extent of clay reduction in the presence of U, reactors began with 1×10^8 CN32 cells/mL, 2.0 g/L NAu-2, 5 mM sodium lactate, and 830 μM uranyl acetate. After 240 h, 850 μM uranyl acetate and 5 mM sodium lactate were added to the reactors by needle and syringe. Control reactors were established by adding only 5 mM sodium lactate to the reactors [and a volume of PB buffer equal to the added volume of U(VI)]. CN32 was not reinoculated into any of these reactors.

To examine the effect of cell viability, reactors were reinoculated with CN32 after 340 h. These experiments began with 1×10^8 CN32 cells/mL, 2.0 g/L NAu-2, and 5 mM sodium lactate [no U(VI) added initially], and then after 340 h, 1×10^8 fresh CN32 cells/mL, 800 μM uranyl acetate, and 5 mM sodium lactate were added to the reactors by needle and syringe. No-reinoculation control reactors were established by adding only 5 mM sodium lactate to the reactors [and a volume of PB buffer equal to the added volumes of CN32 and U(VI)]. No-U(VI) control reactors were established by adding only fresh CN32 and sodium lactate to these reactors [and a volume of PB buffer equal to the added volume of U(VI)].

Abiotic Reduction of Unaltered Nontronite. Biogenic uraninite [UO_2(am)], chemically reduced anthraquinone 2,6-disulfonate (AQDS), and citrate-bicarbonate-dithionite (CBD) were all used to measure the abiotic reduction of clay-Fe(III) in nontronite. Reactors started with ∼15 mL of PB buffer containing 1×10^8 CN32 cells/mL, 830 μM uranyl acetate, and 5 mM sodium lactate. After a 240 h incubation [total U(VI) concentrations were nearly constant after 50 h (Figure 1b)], the cell−uraninite precipitates were pasteurized (75 °C for 60 min, three times over 5 days) to deactivate biological activity. Biological activity was not detected in pasteurized materials added to fresh medium containing U(VI) or nontronite. No attempt was made to remove spent biomass or wash the uraninite precipitates. A needle and syringe were used to add 2.0 g/L NAu-2 to bioreduced, pasteurized suspensions of uraninite [830 μM total U, 83.8% U(IV)] in PB buffer. Reactors were incubated at 100 rpm in the anoxic chamber. Bioreduced, pasteurized suspensions of uraninite with no clay added were prepared as controls. Samples were analyzed[23] for Fe(II) and U(VI) as described below.

Chemically reduced AH_2DS was prepared by bubbling 99.995% H_2 gas into an AQDS solution in the presence of a Pd catalyst (0.5 wt % Pd on 3.2 mm alumina pellets) inside an anoxic chamber.[24] A needle and syringe were used to add NAu-2 (0.25 or 1.0 g/L) to AH_2DS (200, 400, or 800 μM) in deoxygenated 30 mM PIPES buffer (pH 7.0; 100% N_2). Reactors were incubated at 100 rpm in the anoxic chamber. No-clay controls were prepared. Samples were analyzed for Fe(II) and concentrations of AH_2DS/AQDS[13] (described below).

Nontronite (2.0 g/L) was reduced using sodium dithionite (6 g/L) in a sodium citrate (266 mM)/sodium bicarbonate (111 mM) buffer[13,25] at room temperature. No-CBD controls were prepared. Samples were analyzed for Fe(II) as described below.

Analytical Methods. In clay-uranium reaction systems, U and Fe concentrations are difficult to measure because of analytical artifacts caused by U(IV/VI)−Fe(II/III) valence cycling in conventional extraction solutions.[23] Therefore, we developed and validated a sequential acid extraction/mineral digestion method to avoid these types of analytical interference.[23] Suspension samples were extracted in a 1.40 M H_3PO_4/0.50 M H_2SO_4 mixture (final concentrations) for 10 min and then centrifuged at 14100*g* for 10 min. This supernatant was used to measure H_3PO_4/H_2SO_4-extractable Fe(II/III) and H_3PO_4/H_2SO_4-extractable U(IV/VI). Uranium was measured using an anoxic automated KPA method.[23] U(IV/VI) was speciated by analyzing samples and then reanalyzing samples after they had been oxidized with 70% HNO_3 and heated in a boiling water bath for 45 min. The remaining mineral pellet was used to measure H_3PO_4/HF-H_2SO_4-digestable Fe(II/III) using the modified HF-H_2SO_4/phenanthroline digestion method.

In abiotic reduction experiments conducted with AH_2DS and CBD, suspension samples were first centrifuged at 14100*g* for 10 min before clay digestion. This supernatant was used to measure dissolved AH_2DS and AQDS, dissolved Fe(II), and dissolved metals. Dissolved AH_2DS and AQDS concentrations were measured in the anoxic chamber by UV−vis spectrophotometry.[13] Dissolved Fe(II) was measured using the phenanthroline method. The remaining mineral pellet was used to

measure H_3PO_4/HF-H_2SO_4-digestable Fe(II/III) using the modified HF-H_2SO_4/phenanthroline digestion method.[23]

Mössbauer Spectroscopy. Transmission Mössbauer spectroscopy was performed using a SVT400 cryogenic Mössbauer system (SEE Co.). The ^{57}Co (~50 mCi) was in a Rh matrix at room temperature. All hyperfine parameters were reported relative to α-Fe foil at room temperature. Samples were dried and ground to a powder anaerobically and sealed between two pieces of 5 mL kapton tape to avoid oxidation when the sample was transferred from the anoxic chamber to the sample holder. Spectral fitting was conducted using Recoil Software (University of Ottawa, Ottawa, ON). All fits were conducted using a Voigt-based model. The Lorentzian line width was held at 0.14 mm/s during fitting, as it was the line width measured on the spectrometer for an ideally thick α-Fe foil. For all fits, unless otherwise noted, the center shift (CS), quadrupole shift (QS), hyperfine parameter (H), and relative areas between sites were allowed to float during fitting.

Kinetic Analyses. Zero-order reduction rates of U(VI) and clay-Fe(III) were calculated according to

$$k_U = \frac{dU}{dt} = \frac{[U(VI)_0] - [U(VI)_t]}{t} \quad (1)$$

$$k_{Fe} = \frac{dFe}{dt} = \frac{[Fe(II)_t] - [Fe(II)_0]}{t} \quad (2)$$

where k_U and k_{Fe} are the zero-order reduction rates of U(VI) and clay-Fe(III), respectively (micromolar per hour), $U(VI)_0$ is the H_3PO_4/H_2SO_4-extractable U(VI) concentration at time 0 (micromolar), $U(VI)_t$ is the H_3PO_4/H_2SO_4-extractable U(VI) concentration at time t (micromolar), $Fe(II)_t$ is the total Fe(II) concentration (H_3PO_4/H_2SO_4-extractable + H_3PO_4/HF-H_2SO_4-digestable) at time t (micromolar), $Fe(II)_0$ is the total Fe(II) concentration (H_3PO_4/H_2SO_4-extractable + H_3PO_4/HF-H_2SO_4-digestable) at time 0 (micromolar), and t is the reaction time (hours). While initial rates of U(VI) and clay-Fe(III) could have been fit to a first-order rate model, a zero-order rate model was selected because it worked well for both initial fast rates and long-term slow rates. Rates could then be readily compared between different stages of the incubation periods.

RESULTS AND DISCUSSION

Bioreduction of Clay-Fe(III) and U(VI). Nontronite bioreduction experiments were conducted with *S. putrefaciens* CN32 in the presence and absence of U(VI) to determine if U played an active or passive role in clay-Fe(III) reduction (Figure 1). The initial rate of clay-Fe(III) reduction was significantly faster in the presence of U (k_{Fe} = 40.3 μM/h from 0 to 41 h) than in reactors without U (k_{Fe} = 10.7 μM/h from 0 to 41 h) (Table 1). Unlike the rates, however, the final extents of clay-Fe(III) reduction in reactors with U (22.5 ± 0.5%) and without U (22.2 ± 0.1%) were virtually identical. The observation that U enhanced the initial rate of clay-Fe(III) reduction (from 0 to 41 h), but not the final extent, led us to hypothesize that U plays an active role in the bioreduction of clay minerals by serving as an electron shuttle that facilitates the transfer of electrons between CN32 and clay-Fe(III).

We also performed bioreduction experiments of U(VI) in the presence and absence of NAu-2 or aluminum (Al) oxide, with the Al oxide serving as a redox-inactive mineral control to account for U(VI) sorption. The initial rate of U(VI) reduction in the presence of NAu-2 was lower (k_U = 9.49 μM/h from 0 to 41 h) than when NAu-2 was absent (k_U = 17.6 μM/h from 0 to 41 h). The final extent of U(VI) reduction was very similar between the experiments with and without NAu-2 (Figure 1b), indicating that NAu-2 did not influence the extent to which CN32 could reduce U(VI). In the control experiment with Al oxide (Figure S2 of the Supporting Information), the initial rate of U(VI) reduction (k_U = 15.7 μM/h from 0 to 41 h) was very similar to those observed for the reactors containing just U(VI), suggesting that U sorption was not a major influence on U(VI) reduction rates. These observations further supported our hypothesis that U shuttles electrons between CN32 and NAu-2.

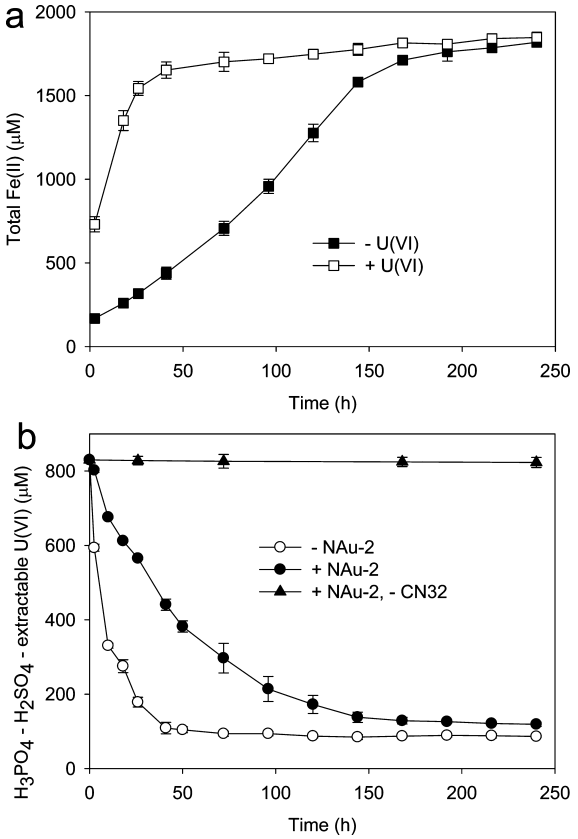

Figure 1. Bioreduction of nontronite NAu-2 and uranium(VI). Experiments conducted with 1 × 10^8 CN32 cells/mL, 2.0 g/L NAu-2, and 830 μM uranyl acetate [U(VI)] in 10 mM PIPES/30 mM $NaHCO_3$ buffer (pH 7.0). (a) Fe(II) concentration vs time. Total Fe(II) = H_3PO_4/H_2SO_4-extractable Fe(II) + HF-H_2SO_4-digestable Fe(II). (b) U(VI) concentration vs time. Symbols represent means of triplicate measurements, and error bars represent one standard deviation.

Furthermore, these findings clearly showed that the bioreduction of U(VI) and clay-Fe(III) by CN32 occurred concomitantly (Figure 1). This observation contradicts a previous study by our group,[19] in which we reported that U(VI) reduction by *Shewanella oneidensis* MR-1 occurred prior to the reduction of structural Fe(III) in NAu-2. It was previously proposed that MR-1 preferentially bioreduced U(VI) over clay-Fe(III) and that U(IV) in the form of uraninite was reoxidized by clay-Fe(III) during the period of U(VI) reduction. Subsequently, it was discovered that this observation was an experimental artifact that arose because of U(IV/VI) and clay-Fe(II/III) valence cycling in the extraction solutions commonly used to measure clay-Fe(II) and U(VI).[23] Since then, we have developed and validated a sequential

dx.doi.org/10.1021/es404885e | Environ. Sci. Technol. 2014, 48, 2750−2758

Table 2. Summary of the Extents of Reduction of Nontronite NAu-2 after Respiking with Various Experimental Components

	preliminary manipulation		respiked components			reduction rate		
	"pre-reduction" incubation (h)	extent of NAu-2 reduction (%) after 240 or 340 h	[CN32] (cells/mL)	U(VI) (μM)	lactate (mM)	time (h)	k (μM/h)	final extent of NAu-2 reduction (%)
Figure S2	240[a]	22.6	0	0	5	240–432	0.90 Fe	24.9 (432 h)[c]
Figure S2	240[a]	22.7	0	850	5	240–432	0.88 Fe	24.9 (432 h)[c]
							4.22 U	
Figure S3	340[b]	24.4	0	0	5	340–484	2.67 Fe	26.9 (484 h)[c]
Figure S3	340[b]	24.5	1×10^8	0	5	340–484	2.58 Fe	30.3 (484 h)[c]
						340–361	34.1 U	
						361–484	0.21 U	
Figure S3	340[b]	24.5	1×10^8	800	5	340–484	1.15 Fe	30.0 (484 h)[c]

[a]With 1×10^8 CN32 cells/mL, 2.0 g/L NAu-2, 5 mM lactate, and 830 μM U(VI) from 0 to 240 h. [b]With 1×10^8 CN32 cells/mL, 2.0 g/L NAu-2, and 5 mM lactate from 0 to 340 h. [c]Total incubation time.

H_3PO_4/H_2SO_4 extraction and HF-H_2SO_4/phenanthroline digestion procedure to avoid this artifact.[23]

In the bioreduction experiments, only a fraction of clay-Fe(III) was reduced. This observation was consistent with several other studies that revealed incomplete clay-Fe(III) reduction using several types of bacteria and clay minerals.[2,12] To understand what factors controlled the extent of clay-Fe(III) reduction, we performed two-stage experiments in which we first conducted bioreduction experiments as described above until clay-Fe(II) concentrations plateaued after approximately 240 or 340 h and then added fresh U(VI), lactate, and/or CN32 to see if these amendments would lead to further clay-Fe(III) reduction (Table 2). Under all the conditions investigated, we observed only a modest increase in the extent of reduction. In reactors amended with additional lactate, the extent of clay-Fe(III) reduction increased slightly from 22.6 ± 0.1% at 240 h to 24.9 ± 1.0% at 432 h (Table 2 and Figure S3 of the Supporting Information). Similarly, amending reactors with fresh CN32 and lactate modestly increased the extent of reduction from 24.5 ± 0.3% at 340 h to 30.3 ± 0.9% at 484 h (Table 2 and Figure S4 of the Supporting Information). In reactors amended with (i) U(VI) and lactate or (ii) CN32, U(VI), and lactate, rapid U(VI) reduction occurred, but the extent of clay-Fe(III) reduction increased by only approximately 6% (Table 2). Collectively, these experiments indicated (i) incomplete clay-Fe(III) reduction was not due to a loss of CN32 viability and (ii) the addition of U did not influence the final extent of clay-Fe(III) reduction. Instead, these results suggest that the partial reduction of clay-Fe(III) was caused by thermodynamic constraints, as discussed in more detail below.

Bioreduction of Clay-Fe(III) and AQDS. Bioreduction experiments were performed with AQDS and NAu-2 in the absence of U to quantify the effect of a completely soluble electron shuttle on the kinetics and extent of clay-Fe(III) bioreduction by CN32. The initial zero-order rates of clay-Fe(III) reduction (k_{Fe}) increased from 20.1 μM/h (from 0 to 96 h) in the absence of AQDS to 27.7 μM/h (from 0 to 96 h) in the presence of AQDS (Table 1). In contrast to these kinetic observations, the presence of AQDS did not affect the final extent of clay-Fe(III) reduction (Figure 2). The final extents of clay-Fe(III) reduction after 900 h were 34.5 ± 0.6 and 35.9 ± 1.4% in the absence and presence of AQDS, respectively, an insignificant difference ($p > 0.1$). There are discrepancies in the literature where electron shuttles have been shown to enhance both the rate and extent of clay-Fe(III) reduction.[13−15] Our results are consistent with a recent study of the bioreduction of clay-Fe(III) by a thermophilic methanogen, *Methanothermobacter thermautotrophicus*, in which AQDS enhanced only the rate of clay-Fe(III) reduction and not the final extent.[16] Discrepancies in the literature are likely caused in part by differences in incubation times.

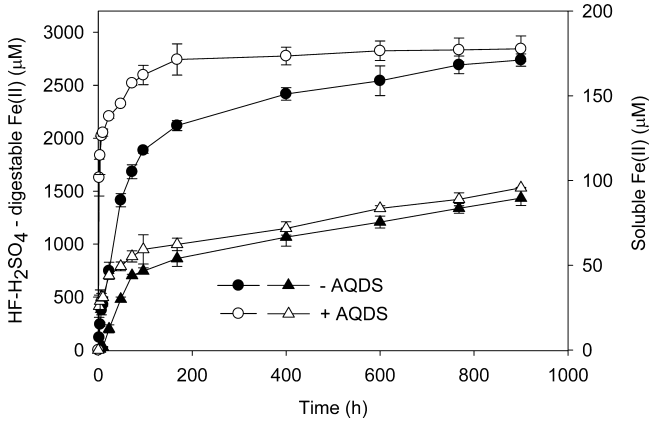

Figure 2. Bioreduction of nontronite NAu-2 and AQDS. Experiments conducted with 1×10^8 CN32 cells/mL, 2.0 g/L NAu-2, and 0.1 mM AQDS in 10 mM PIPES/30 mM $NaHCO_3$ buffer (pH 7.0). Circles represent HF-H_2SO_4-digestable Fe(II) and triangles soluble Fe(II), and filled symbols are for experiments conducted in the absence of AQDS. Symbols represent means of triplicate measurements, and error bars represent one standard deviation.

Mössbauer spectroscopy (MBS) was used to provide an additional measure of the extent of clay-Fe(III) reduction (Figure S1 of the Supporting Information). Mössbauer spectra were collected for a subset of the samples to confirm that the H_3PO_4/H_2SO_4 extraction and HF-H_2SO_4/phenanthroline digestion procedures were not affected by analytical artifacts (Table S1 of the Supporting Information). Excellent agreement was found between the extents of reduction for these two independent methods. For example, the extent of clay-Fe(III) reduction for one bioreduced sample was 34.5% based on our wet chemical procedures and 32.3% based on MBS.

Abiotic Reduction of Clay-Fe(III). Two possibilities may explain why CN32 was capable of reducing only a fraction of the clay-Fe(III). (i) Only a fraction of the structural Fe was bioaccessible to the CN32, or (ii) the extent of reduction was limited by thermodynamic constraints [i.e., it became energetically unfavorable for CN32 to use clay-Fe(III) as an electron acceptor]. To address this question, we performed abiotic clay-Fe(III) reduction experiments using three chemical reductants: AH_2DS, uraninite, and dithionite.

For the AH_2DS experiments, batch reactors were prepared with varied concentrations of NAu-2 (0.25 or 1.0 g/L) and AH_2DS (200−800 μM). These experiments were designed to yield measurable concentrations of all products and reactants such that an electron balance between clay-Fe(II) produced and AH_2DS consumed could be determined. In all the AH_2DS experiments, the extent of clay-Fe(III) reduction was repeatedly limited to 18.0−19.0% after 120 h (Figure 3). Measurements confirmed the theoretical stoichiometric ratio of 2 mol of Fe(II) produced/mol of AH_2DS consumed (Figure S5 of the Supporting Information). Because excess AH_2DS remained at the end of these experiments and the final concentrations of AH_2DS were nearly constant, these results indicated that AH_2DS was not a sufficiently strong reductant to reduce the remaining clay-Fe(III).

For the uraninite experiments, batch reactors were prepared with varied concentrations of NAu-2 (0.25 or 2.0 g/L) and uraninite (330 or 830 μM). In all of these experiments, measurements confirmed the theoretical stoichiometric ratio of 2 mol of Fe(II) produced/mol of U(VI) produced (Figure 4c). In experiments conducted with 0.25 g/L NAu-2 and 330 μM uraninite, excess uraninite remained after incubation for 80 days (kinetic data not shown). Under these conditions, the extent of reduction of clay-Fe(III) reached only 16.4%. Similar to the AH_2DS experiments, excess reductant remained at the end of these experiments, yet clay-Fe(III) reduction essentially ceased. These results suggest that uraninite, like AH_2DS, was not a sufficiently strong reductant to reduce the remaining clay-Fe(III).

For the dithionite experiments, batch reactors with 2.0 g/L NAu-2 were reacted with CBD (6 g/L sodium dithionite) at room temperature. Unlike reactions with AH_2DS or uraninite, NAu-2 was nearly completely reduced [91.5% clay-Fe(II)] after incubation for 20 days (Figure S6 of the Supporting Information). This high extent of reduction of NAu-2 by dithionite was consistent with previous studies.[13,25] The difference between the extents of reduction achieved with CN32 (22.2−35.9%) and those achieved with dithionite provides strong evidence that the biological extent of reduction was thermodynamically limited.

Thermodynamic Considerations. To evaluate if clay-Fe(III) reduction was limited by thermodynamics, we constructed a model to calculate the reduction potential of the various reactions at their final extents. For each half-cell reaction, the non-standard state reduction potential at pH 7.0 (E'_H) was calculated on the basis of published thermodynamic data (Table 3), the measured final extents of the reduced and oxidized species in the half-cell reaction, and a H^+ concentration of 10^{-7} mol/L according to

$$E'_H = E^\circ_H - 2.303 \times RT/nF \times \log([red]/[ox]) \quad (3)$$

where E°_H is the standard state reduction potential (volts), R is the universal gas constant (joules per mole per kelvin), T is the absolute temperature (kelvin), n is the stoichiometry of electron transfer between the oxidized and reduced species, F is the Faraday constant (coulombs per mole), [red] is the chemical activity of the reduced species, [ox] is the chemical activity of the oxidized species, and $[H^+]$ would be included depending on the form of the balanced half-cell reaction. The overall non-standard state reduction potential at pH 7.0 ($E'_{H,overall}$) was then calculated according to

$$E'_{H,overall} = E'_{H,oxidant} - E'_{H,reductant} \quad (4)$$

where $E'_{H,oxidant}$ is the value calculated from eq 3 for the oxidant in the overall balanced redox reaction at pH 7.0 (volts) and $E'_{H,reductant}$ is the value calculated from eq 3 for the reductant in the overall balanced redox reaction at pH 7.0 (volts).

In all of these abiotic experiments and for all of these calculations, clay-Fe(III) served as the oxidant. Recently, our

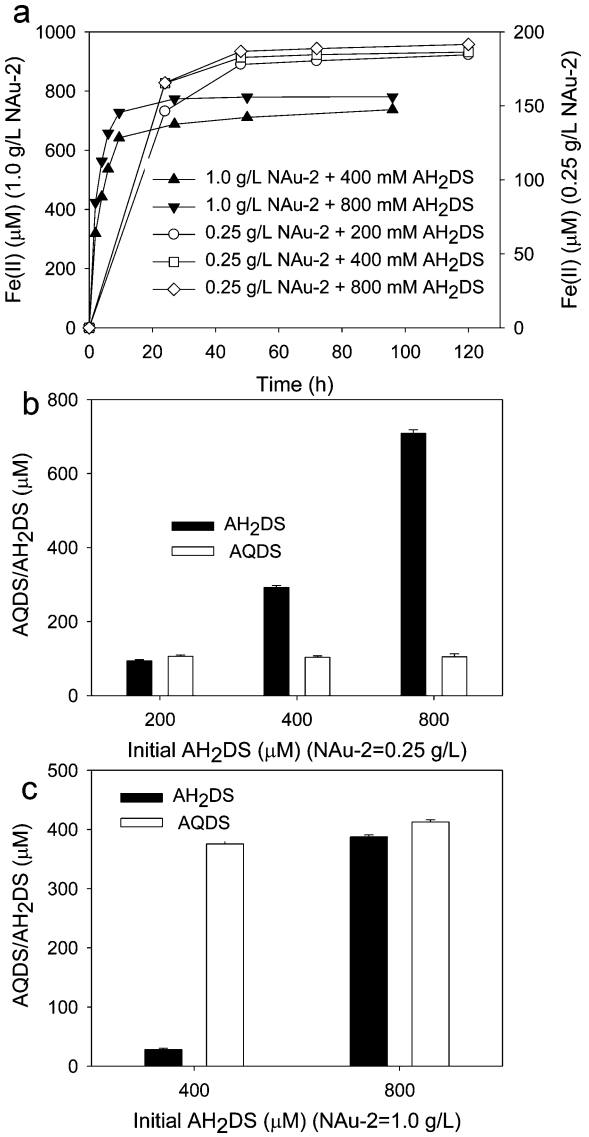

Figure 3. Abiotic reduction of nontronite NAu-2 by AH_2DS. (a) Fe(II) concentration vs time. Fe(II) = HF-H_2SO_4-digestable Fe(II). Experiments conducted with 0.25 or 1.0 g/L NAu-2 and 200−800 μM AH_2DS. (b) Final concentrations of AH_2DS and AQDS for experiments conducted with 0.25 g/L NAu-2 and 200−800 μM AH_2DS. (c) Final concentrations of AH_2DS and AQDS for experiments conducted with 1.0 g/L NAu-2 and 400−800 μM AH_2DS.

dx.doi.org/10.1021/es404885e | Environ. Sci. Technol. 2014, 48, 2750−2758

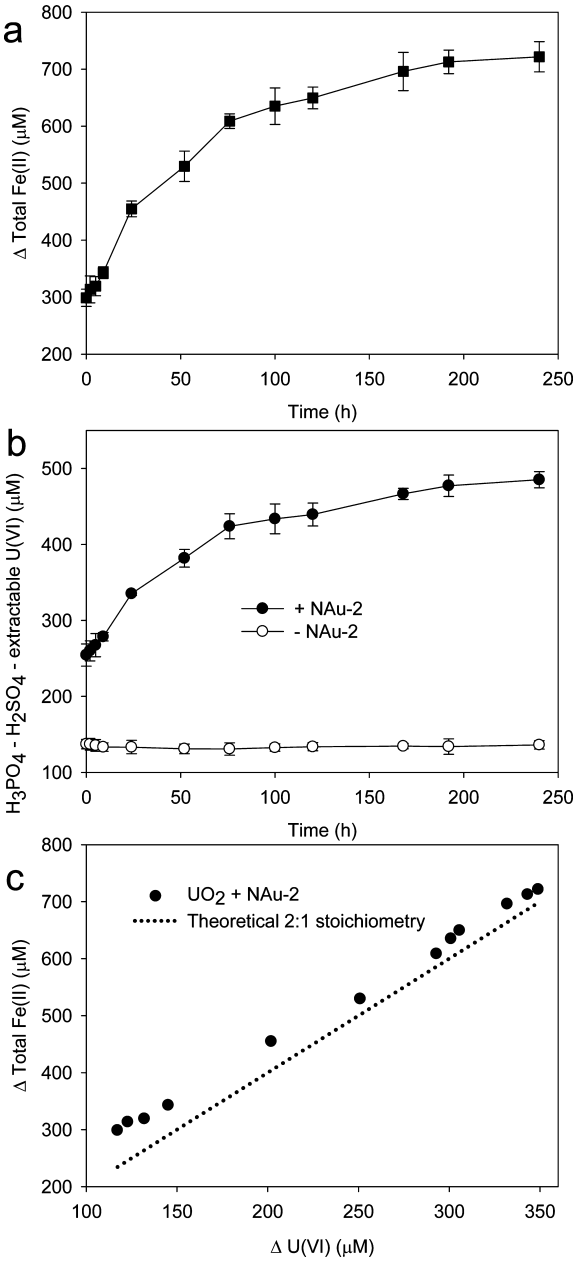

Figure 4. Abiotic reduction of nontronite NAu-2 by biogenic uraninite. Experiments conducted with 830 μM bioreduced uraninite [83.8% U(IV)] and 2.0 g/L NAu-2 in 10 mM PIPES/30 mM $NaHCO_3$ buffer (pH 7.0). (a) Fe(II) concentration vs time. Total Fe(II) = H_3PO_4/H_2SO_4-extractable Fe(II) + HF-H_2SO_4-digestable Fe(II). (b) U(VI) concentration vs time. (c) Stoichiometric relationship between Δmoles of Fe(II) and Δmoles of U(VI). $[\Delta\text{Total Fe(II)}] = [\text{Total Fe(II)}]_t - [\text{Total Fe(II)}]_{t=0}$. $[\Delta\text{U(VI)}] = [\text{U(VI) + NAu-2}]_t - [\text{U(VI) − NAu-2}]_t$. The dotted line represents the theoretical stoichiometry of 2 mol of Fe(II)/mol of U(VI). Symbols represent means of triplicate measurements, and error bars represent one standard deviation.

group measured the clay-Fe(II):Fe(III) ratios for NAu-2 as a function of E'_H at pH 7.5 using mediated electrochemical reduction,[20] a technique that uses soluble electron-mediating compounds to facilitate electron transfer between structural Fe in suspended clay mineral particles and a working electrode set to a constant applied E'_H.[26,27] In this work, we found that NAu-2 and other commonly studied smectites do not exhibit a single

Table 3. Standard State Reduction Potentials ($E°_H$) and Standard State Reduction Potentials at pH 7.0 ($E°'_H$) for Redox-Active Materials Used in This Study

reaction	$E°_H$ (V)	$E°'_H$ (V)
nontronite NAu-2		
clay-Fe(III)(s) + e^- + H^+(aq) → clay-Fe(II)-H(s)		−0.34[a]
uranyl carbonate		
$0.5UO_2(CO_3)^{4-}_3$(aq) + $1.5H^+$(aq) + e^- → $0.5UO_2$(s) + $1.5HCO^-_3$(aq)	0.40[b]	−0.22[b]
uranyl carbonate		
$0.5UO_2(CO_3)^{4-}_3$(aq) + $1.5H^+$(aq) + e^- → $0.5UO_2$(s) + $1.5HCO^-_3$(aq)	0.53[c]	−0.09[c]
anthraquinone 2,6-disulfonate		
0.5AQDS(aq) + H^+(aq) + e^-(aq) → $0.5AH_2DS$(aq)	0.23[d]	−0.18
Shewanella heme proteins		−0.15 to −0.32[e,f]
sodium dithionite		−0.44[g] to −0.66[h]

[a]From work by C. A. Gorski et al. (submitted to *Environmental Science & Technology*) with respect to eq 5 and with β = 0.36. [b]$\Delta G_f°$ = −1003.6 kJ/mol for UO_2(am). [c]$\Delta G_f°$ = −977 kJ/mol for UO_2(am).[30] [d]From ref 35. [e]From ref 31. [f]From ref 32. [g]From ref 34. [h]From ref 33.

$E°'_H$; instead, clay-Fe(II)/Fe(III) redox couples are redox-active over a range of E'_H values much wider than what would be expected for a single Fe(II)/Fe(III) redox couple. To account for this broadening, we fit the NAu-2 redox profile using a modified Nernst equation:[20]

$$E'_H = E°'_{H,\text{NAu-2}} - (1/\beta) \times 2.303RT/nF \times \log([\text{clay-Fe(II)}]/[\text{clay-Fe(III)}]) \quad (5)$$

where β is a dimensionless factor used to describe the broadening of the $E°'_H$ values (unique for each smectite), [clay-Fe(II)] is the concentration of structural clay-Fe(II) (moles per liter), and [clay-Fe(III)] is the concentration of structural clay-Fe(III) (moles per liter). The dimensionless factor β ranges from 0 to ≤1 with values smaller than unity resulting in a widened E'_H range over which electrons are accepted and donated relative to the ideal Nernst case (i.e., β = 1). For these calculations, we assumed that the chemical activities of clay-Fe(II) and clay-Fe(III) were equal to their measured concentrations in suspension. For nontronite NAu-2 at pH 7.0, E'_H values were calculated using an $E°'_H$ of −0.34 V and a β of 0.36.[20]

The values of $E'_{H,\text{reductant}}$ for AH_2DS and uraninite were calculated using published thermodynamic data (Table 3) and measured final concentrations. At pH 7.0, the predominant reduced species of AQDS is AH_2DS such that $E°'_H$ was calculated to equal −0.18 V, consistent with previous reports.[28] At pH 7.0 in PB buffer, speciation modeling using Minteq[29] showed that $UO_2(CO_3)_3^{4-}$ was the predominant U(VI) species in the abiotic reduction experiments. Reported values for the free energy of formation ($\Delta G_f°$) of UO_2(am) range from −977 to −1004 kJ/mol.[30] The less negative $\Delta G_f°$ corresponded to a more amorphous form of uraninite. Details of our calculations of $E°'_H$ for the uraninite/$UO_2(CO_3)_3^{4-}$ half-cell reaction are included in the Supporting Information. The E'_H of the uraninite/$UO_2(CO_3)_3^{4-}$ half-cell reaction was calculated assuming that the activity of uraninite was unity and the activity of $UO_2(CO_3)_3^{4-}$ was equal to the U(VI) concentration measured in suspension (moles per liter).

Using these values for $E'_{H,oxidant}$ and $E'_{H,reductant}$ (Tables S3 and S4 of the Supporting Information), we found that the final extents of these reactions were reasonably close to $E'_{H,overall} = 0$, supporting our assumption that these experiments had reached an "apparent equilibrium" condition. For the NAu-2 and AH_2DS experiments (Figure 3), $E'_{H,overall}$ values ranged from −0.03 to −0.08 V. For the NAu-2 and uraninite experiment, the $E'_{H,overall}$ values ranged from −0.04 to −0.17 V, based on ΔG_f° values for UO_2(am) of −977 and −1004 kJ/mol, respectively.[30] Because of the amorphous nature and small particle size associated with biogenic uraninite produced by CN32,[19] a ΔG_f° for UO_2(am) of −977 kJ/mol is arguably most appropriate for our experimental conditions and yielded an $E'_{H,overall}$ of −0.04 V.

Our results suggest that thermodynamics factor into the extent of clay reduction and may be used to explain differences in the extents of reduction by different microorganisms or differences among clay mineral samples.[12] In Figure 5, reported values of $E^{\circ\prime}_{H,reductant}$ for the reductants used in this study (AH_2DS, CN32, dithionite, and uraninite) are plotted versus the final extent of clay-Fe(III) reduction measured in our experiments. $E^{\circ\prime}_{H,reductant}$ values for *Shewanella* spp. refer to specific proteins involved in the transport of electrons to metal oxides.[31,32] The symbol shown in Figure 5 for *Shewanella* is the mean value calculated from four specific proteins (CymA and OmcA;[31] Sffcc3 and Sofcc3[32]), and the error bars represent the reported range of reduction potentials at pH 7.0. $E^{\circ\prime}_{H,reductant}$ values for dithionite are reported from −0.47 to −0.66 V.[33,34] The $E^{\circ\prime}_{H,oxidant}$ values for clay-Fe(II/III) in NAu-2 were calculated using eq 5 with an $E^{\circ\prime}_H$ of −0.34 V and a β of 0.36 as independently determined from mediated electrochemical reduction.[20] This trend establishes a way to visualize the thermodynamic relationship between the strength of the reductant and the final extent of clay-Fe(III) reduction. The clay-Fe(III) reduction extent plotted for the *Shewanella* proteins was from the longest-term incubation experiments (900 h) (Table 1). These data demonstrate that the extent of clay-Fe(III) reduction is controlled by the strongest reductant in an environmental system. For example, in abiotic experiments conducted with AH_2DS or uraninite, the extent of clay-Fe(III) reduction was always greater in the presence of CN32. These results suggest that at least one protein in CN32 involved in the transfer of electrons to clay-Fe(III) could achieve a lower reduction potential than AH_2DS or uraninite.

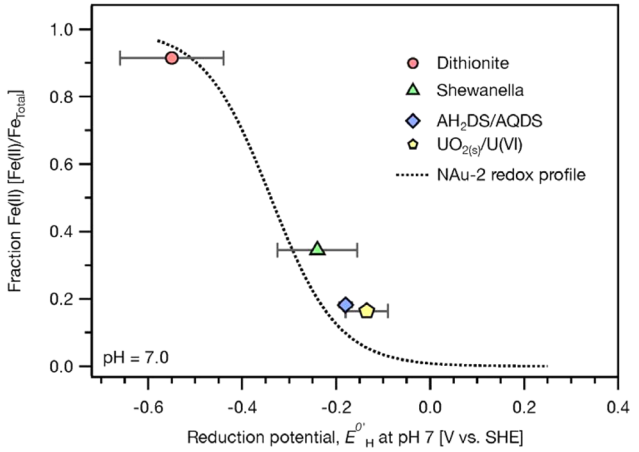

Figure 5. Measured fractions of Fe(II) vs reported standard state reduction potential values at pH 7.0 ($E^{\circ\prime}_H$) for the four reductants investigated in this study. The reduction potential values were calculated from literature sources in Table 3. Error bars represent the reported range of $E^{\circ\prime}_H$ values. The dashed line is the fitted $E^{\circ\prime}_H$ profile for clay-Fe(II/III) in nontronite NAu-2 as determined by mediated electrochemical reduction.[20]

The rates and extents of clay-Fe(III) reduction achieved with CN32 (Figures 1 and 2), AH_2DS (Figure 3), and uraninite (Figure 4) can be synthesized to posit a mechanistic description of the transfer of an electron to structural clay-Fe(III). First, soluble electron shuttles such as AQDS or an analogous compound produced by CN32 deliver their electrons to clay-Fe(III) at a rate that is greater than the rate of electron transfer between solid-phase uraninite and clay-Fe(III). Second, the first ∼20% of clay-Fe(III) in nontronite NAu-2 was relatively easy (i.e., rapid) to reduce; the next 15% of clay-Fe(III) was harder to reduce (i.e., kinetic limitation), and the remaining 65% of clay-Fe(III) was effectively biologically unreducible (i.e., thermodynamic limitation). Third, a small (∼1%) but highly reactive fraction of structural clay-Fe(III) was readily dissolved after reduction (Figure 2). Importantly, we show that the concomitant bioreduction of U(VI) and clay-Fe(III) will likely occur in the subsurface. These processes would be consistent with field observations where U is found to accumulate in reduced, clay-rich sediments. Our thermodynamic model should be able to predict the extent of reduction of clay-Fe(III) under a wide variety of environmental conditions.

■ ASSOCIATED CONTENT

Supporting Information

Mössbauer spectroscopy (Figure S1 and Table S1), thermodynamic calculations (Tables S2−S4), bioreduction data (Figures S2−S4), and abiotic reduction data (Figures S5 and S6). This material is available free of charge via the Internet at http://pubs.acs.org.

■ AUTHOR INFORMATION

Corresponding Author

*Department of Civil and Environmental Engineering, The Pennsylvania State University, 212 Sackett Building, University Park, PA 16802. E-mail: wdb3@psu.edu. Phone: (814) 863-0578. Fax: (814) 863-7304.

Notes

The authors declare no competing financial interest.

■ ACKNOWLEDGMENTS

We thank Aron Griffin (The Pennsylvania State University) for helping with the collection of Mössbauer spectra and modeling. This research was supported by the Subsurface Biogeochemical Research (SBR) Program, Office of Science (BER), U.S. Department of Energy (DOE), Grant DE-SC0005333 to The Pennsylvania State University.

■ REFERENCES

(1) Amonette, J. E., Fitch, A., Eds. Iron redox chemistry of clays and oxides: Environmental applications. *Electrochemical properties of clays*; Clay Minerals Society: Chantilly, VA, 2002; pp 89−147.

(2) Lee, K.; Kostka, J. E.; Stucki, J. W. Comparisons of structural Fe reduction in smectites by bacteria and dithionite: An infrared spectroscopic study. *Clay Clay Miner.* **2006**, *54* (2), 195−208.

(3) Brigatti, M. F.; Franchini, G.; Lugli, C.; Medici, L.; Poppi, L.; Turci, E. Interaction between aqueous chromium solutions and layer silicates. *Appl. Geochem.* **2000**, *15* (9), 1307−1316.

(4) Hofstetter, T. B.; Neumann, A.; Schwarzenbach, R. P. Reduction of nitroaromatic compounds by Fe(II) species associated with iron-rich smectites. *Environ. Sci. Technol.* **2006**, *40* (1), 235−242.
(5) Neumann, A.; Hofstetter, T. B.; Skarpeli-Liati, M.; Schwarzenbach, R. P. Reduction of polychlorinated ethanes and carbon tetrachloride by structural Fe(II) in smectites. *Environ. Sci. Technol.* **2009**, *43* (11), 4082−4089.
(6) Ilton, E. S.; Haiduc, A.; Moses, C. O.; Heald, S. M.; Elbert, D. C.; Veblen, D. R. Heterogeneous reduction of uranyl by micas: Crystal chemical and solution controls. *Geochim. Cosmochim. Acta* **2004**, *68* (11), 2417−2435.
(7) Lee, J. H.; Fredrickson, J. K.; Kukkadapu, R. K.; Boyanov, M. I.; Kemner, K. M.; Lin, X. J.; Kennedy, D. W.; Bjornstad, B. N.; Konopka, A. E.; Moore, D. A.; Resch, C. T.; Phillips, J. L. Microbial reductive transformation of phyllosilicate Fe(III) and U(VI) in fluvial subsurface sediments. *Environ. Sci. Technol.* **2012**, *46* (7), 3721−3730.
(8) Komlos, J.; Peacock, A.; Kukkadapu, R. K.; Jaffe, P. R. Long-term dynamics of uranium reduction/reoxidation under low sulfate conditions. *Geochim. Cosmochim. Acta* **2008**, *72* (15), 3603−3615.
(9) Gorby, Y. A.; Lovley, D. R. Enzymatic uranium precipitation. *Environ. Sci. Technol.* **1992**, *26* (1), 205−207.
(10) Senko, J. M.; Istok, J. D.; Suflita, J. M.; Krumholz, L. R. In-situ evidence for uranium immobilization and remobilization. *Environ. Sci. Technol.* **2002**, *36* (7), 1491−1496.
(11) Wu, W.-M.; Carley, J.; Gentry, T.; Ginder-Vogel, M. A.; Fienen, M.; Mehlhorn, T.; Yan, H.; Caroll, S.; Pace, M. N.; Nyman, J.; Luo, J.; Gentile, M. E.; Fields, M. W.; Hickey, R. F.; Gu, B.; Watson, D.; Cirpka, O. A.; Zhou, J.; Fendorf, S.; Kitanidis, P. K.; Jardine, P. M.; Criddle, C. S. Pilot-scale in situ bioremedation of uranium in a highly contaminated aquifer. 2. Reduction of U(VI) and geochemical control of U(VI) bioavailability. *Environ. Sci. Technol.* **2006**, *40* (12), 3986−3995.
(12) Dong, H. L.; Jaisi, D. P.; Kim, J.; Zhang, G. X. Microbe-clay mineral interactions. *Am. Mineral.* **2009**, *94* (11−12), 1505−1519.
(13) Jaisi, D. P.; Dong, H. L.; Liu, C. X. Influence of biogenic Fe(II) on the extent of microbial reduction of Fe(III) in clay minerals nontronite, illite, and chlorite. *Geochim. Cosmochim. Acta* **2007**, *71* (5), 1145−1158.
(14) Dong, H. L.; Kukkadapu, R. K.; Fredrickson, J. K.; Zachara, J. M.; Kennedy, D. W.; Kostandarithes, H. M. Microbial reduction of structural Fe(III) in illite and goethite. *Environ. Sci. Technol.* **2003**, *37* (7), 1268−1276.
(15) Zhang, J.; Dong, H. L.; Liu, D.; Fischer, T. B.; Wang, S.; Huang, L. Q. Microbial reduction of Fe(III) in illite-smectite minerals by methanogen *Methanosarcina mazei*. *Chem. Geol.* **2012**, *292*, 35−44.
(16) Zhang, J.; Dong, H. L.; Liu, D.; Agrawal, A. Microbial reduction of Fe(III) in smectite minerals by thermophilic methanogen *Methanothermobacter thermautotrophicus*. *Geochim. Cosmochim. Acta* **2013**, *106*, 203−215.
(17) Ribeiro, F. R.; Fabris, J. D.; Kostka, J. E.; Komadel, P.; Stucki, J. W. Comparisons of structural iron reduction in smectites by bacteria and dithionite: II. A variable-temperature Mossbauer spectroscopic study of Garfield nontronite. *Pure Appl. Chem.* **2009**, *81* (8), 1499−1509.
(18) Neumann, A.; Hofstetter, T. B.; Lussi, M.; Cirpka, O. A.; Petit, S.; Schwarzenbach, R. P. Assessing the redox reactivity of structural iron in smectites using nitroaromatic compounds as kinetic probes. *Environ. Sci. Technol.* **2008**, *42* (22), 8381−8387.
(19) Zhang, G. X.; Senko, J. M.; Kelly, S. D.; Tan, H.; Kemner, K. M.; Burgos, W. D. Microbial reduction of iron(III)-rich nontronite and uranium(VI). *Geochim. Cosmochim. Acta* **2009**, *73* (12), 3523−3538.
(20) Gorski, C. A.; Klupfel, L. E.; Voegelin, A.; Sander, M.; Hofstetter, T. B. Redox properties of structural Fe in clay minerals: 3. Relationships between smectite redox and structural properties. *Environ. Sci. Technol.* **2013**, *47* (23), 13477−13485.
(21) Senko, J. M.; Kelly, S. D.; Dohnalkova, A. C.; McDonough, J. T.; Kemner, K. M.; Burgos, W. D. The effect of U(VI) bioreduction kinetics on subsequent reoxidation of biogenic U(IV). *Geochim. Cosmochim. Acta* **2007**, *71* (19), 4644−4654.
(22) Keeling, J. L.; Raven, M. D.; Gates, W. P. Geology and characterization of two hydrothermal nontronites from weathered metamorphic rocks at the Uley Graphite Mine, South Australia. *Clay Clay Miner.* **2000**, *48* (5), 537−548.
(23) Luan, F. B.; Burgos, W. D. Sequential extraction method for determination of Fe(II/III) and U(IV/VI) in suspensions of iron-bearing phyllosilicates and uranium. *Environ. Sci. Technol.* **2012**, *46* (21), 11995−12002.
(24) Boyanov, M. I.; Fletcher, K. E.; Kwon, M. J.; Rui, X.; O'Loughlin, E. J.; Loffler, F. E.; Kemner, K. M. Solution and microbial controls on the formation of reduced U(IV) species. *Environ. Sci. Technol.* **2011**, *45* (19), 8336−8344.
(25) Stucki, J. W.; Golden, D. C.; Roth, C. B. Preparation and handling of dithionite-reduced smectite suspensions. *Clay Clay Miner.* **1984**, *32* (3), 191−197.
(26) Gorski, C. A.; Aeschbacher, M.; Soltermann, D.; Voegelin, A.; Baeyens, B.; Fernandes, M. M.; Hofstetter, T. B.; Sander, M. Redox properties of structural Fe in clay minerals. 1. Electrochemical quantification of electron-donating and -accepting capacities of smectites. *Environ. Sci. Technol.* **2012**, *46* (17), 9360−9368.
(27) Gorski, C. A.; Klupfel, L.; Voegelin, A.; Sander, M.; Hofstetter, T. B. Redox properties of structural Fe in clay minerals. 2. Electrochemical and spectroscopic characterization of electron transfer irreversibility in ferruginous smectite, SWa-1. *Environ. Sci. Technol.* **2012**, *46* (17), 9369−9377.
(28) Fultz, M. L.; Durst, R. A. Mediator compounds for the electrochemical study of biological redox systems: A compilation. *Anal. Chim. Acta* **1982**, *140* (1), 1−18.
(29) Allison, J. D.; Brown, D. S.; Nova-Gradac, K. J. *MINTEQA2/PRODEFA2, a geochemical assessment model for environmental systems: Version 3.0 user's manual*; U.S. Environmental Protection Agency: Athens, GA, 1991.
(30) Guillaumont, R.; Fanghanel, T.; Neck, V.; Fuger, J.; Palmer, D. A.; Grenthe, I.; Rand, M. H. Update on the chemical thermodynamics of uranium, neptumium, plutonium, americium, and technetium; Elsevier B.V.: Amsterdam, 2003.
(31) Field, S. J.; Dobbin, P. S.; Cheesman, M. R.; Watmough, N. J.; Thomson, A. J.; Richardson, D. J. Purification and magneto-optical spectroscopic characterization of cytoplasmic membrane and outer membrane multiheme c-type cytochromes from *Shewanella frigidimarina* NCIMB400. *J. Biol. Chem.* **2000**, *275* (12), 8515−8522.
(32) Pessanha, M.; Rothery, E. L.; Miles, C. S.; Reid, G. A.; Chapman, S. K.; Louro, R. O.; Turner, D. L.; Salgueiro, C. A.; Xavier, A. V. Tuning of functional heme reduction potentials in *Shewanella* fumarate reductases. *Biochim. Biophys. Acta* **2009**, *1787* (2), 113−120.
(33) Mayhew, S. G. Redox potential of dithionite and SO_2^- from equilibrium reactions with flavodoxins, methyl viologen and hydrogen plus hydrogenase. *Eur. J. Biochem.* **1978**, *85* (2), 535−547.
(34) Burton, K. Free energy data of biological interest. *Ergeb. Physiol., Biol. Chem. Exp. Pharmakol.* **1957**, *49*, 275−298.
(35) Clark, W. M. *Oxidation-Reduction Potentials of Organic Systems*; The Williams and Wilkins Co.: Baltimore, 1960.

SUPPORTING INFORMATION

Thermodynamic controls on the microbial reduction of iron-bearing nontronite and uranium

Fubo Luan[1], Christopher A. Gorski[1] and William D. Burgos[1]*

[1]Department of Civil and Environmental Engineering, The Pennsylvania State University, University Park, PA 16801-1408

*Corresponding author: William D. Burgos, Dept. of Civil and Environmental Engineering, The Pennsylvania State University, 212 Sackett Building, University Park, PA, 16802

phone: 814-863-0578; fax: 814-863-7304. Email: wdb3@psu.edu.

Contents

SI-1 Mössbauer Spectroscopy

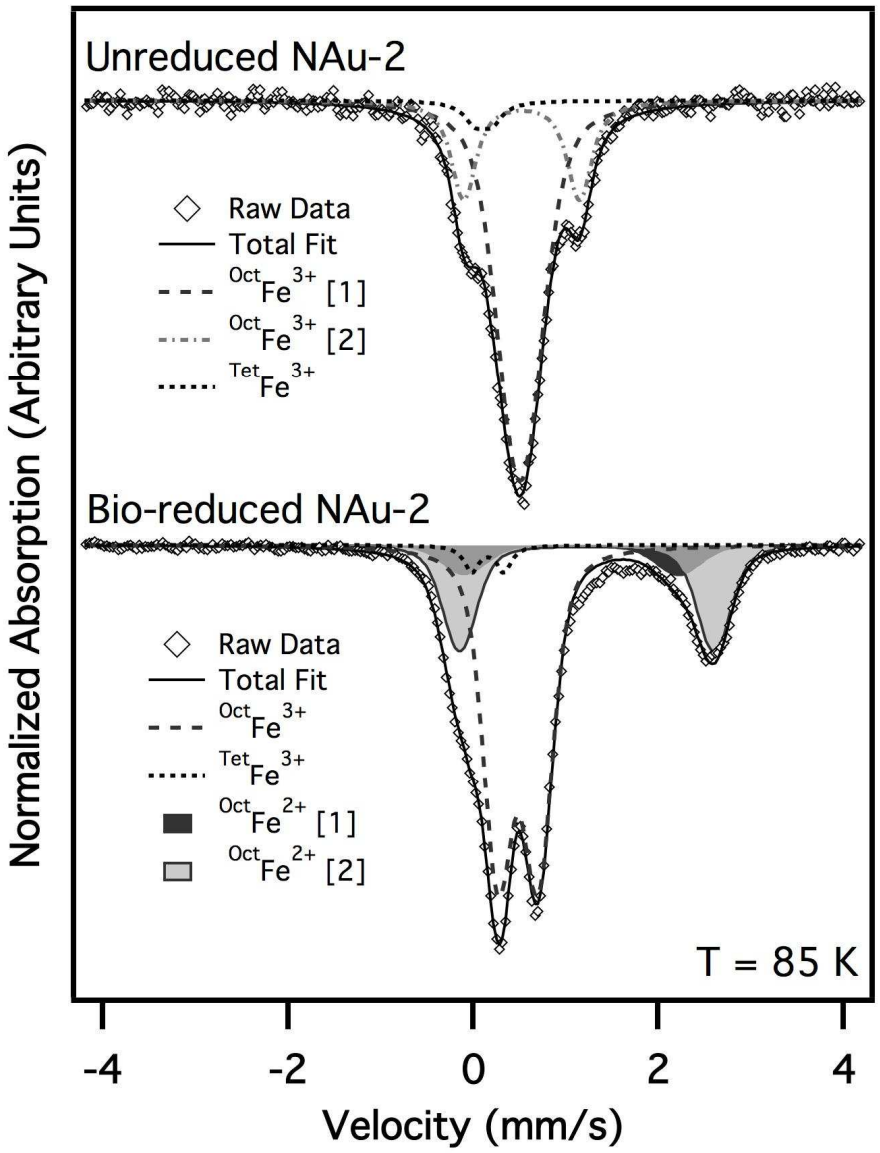

Figure S1. ^{57}Fe Mössbauer spectra collected for the native and bioreduced NAu-2 samples at 85 K. $^{Oct}Fe^{3+}$ = octahedral Fe(III), $^{Tet}Fe^{3+}$ = tetrahedral Fe(III), and $^{Oct}Fe^{2+}$ = octahedral Fe(II). Bracketed numbers shown after site assignments indicate that multiple distinct sites were found for the phase. Fitted hyperfine parameters and relative areas of each site are provided below in Table S1.

Table S1 Mossbauer fitted hyperfine parameters for spectra shown in Figure 3 of the main text. Both spectra were collected at T = 85 K. CS = center shift, QS = quadrupole split, and RA = relative phase abundance in %. Site assignments were done comparing the fitted hyperfine parameters to known ranges for clay-Fe. [A]

Sample	CS, mm/s	QS, mm/s	Phase	RA (%)
Native NAu-2	0.51	0.28	Octahedral Clay-Fe(III)	71.9
	0.52	1.25	Octahedral Clay-Fe(III) [2]	23.7
	0.11	0.18	Tetrahedral Clay-Fe(III)	4.4
Bioreduced NAu-2	1.06	2.33	Octahedral Clay-Fe(II)	8.5
	1.23	2.75	Octahedral Clay-Fe(II) [2]	23.8
	0.48	0.44	Octahedral Clay-Fe(III)	64.5
	0.16	0.35	Tetrahedral Clay-Fe(III)	3.2

[A] http://www.amazon.com/M%C3%B6ssbauer-Spectroscopy-Environmental-Industrial-Utilization/dp/1402077262

SI-2 Thermodynamic Calculations

$$E'_H = E^0_H - 2.303*RT/nF*\log([red]/[ox]) \quad \text{(Eq. 3 from main text)}$$

where, E'_H is the non-standard state reduction potential at pH 7.0, E^0_H is the standard state reduction potential (V), R is the universal gas constant (J mol^{-1} K^{-1}), T is the absolute temperature (K), n is the stoichiometry of electron transfer between the oxidized and reduced species, F is the Faraday constant (C mol^{-1}), [red] is the chemical activity of the reduced species, [ox] is the chemical activity of the oxidized species, and [H^+] would be included depending on the form of the balanced half-cell reaction. The overall non-standard state reduction potential at pH 7.0 ($E'_{H,overall}$) was then calculated according to:

$$E'_{H,overall} = E'_{H,oxidant} - E'_{H,reductant} \quad \text{(Eq. 4 from main text)}$$

where, $E'_{H,oxidant}$ is the value calculated from Eq. 3 for the oxidant in the overall balanced redox reaction at pH 7.0 (V), and $E'_{H,reductant}$ is the value calculated from Eq. 3 for the reductant in the overall balanced redox reaction at pH 7.0 (V).

In analyzing all the abiotic reduction experiments, clay-Fe(III) in nontronite NAu-2 was the oxidant, and uraninite or AH_2DS was the reductant. $E'_{H,oxidant}$ was calculated according to:

$$E'_{H,oxidant} = E^{0\prime}_{H,NAu\text{-}2} - (1/\beta)*2.303*RT/nF*\log([clay\text{-}Fe(II)]/[clay\text{-}Fe(III)])$$

with $E^{0\prime}_{H,NAu\text{-}2}$ = -0.34 V and β = 0.36. As example, insert measured values for [clay-Fe(II)] and [clay-Fe(III)] from end of 80 d uraninite oxidation experiment (Table S3):

$E'_{H,oxidant} = -0.34 - (1/0.36)*(0.059/1)*\log(336*10^{-6}/1714*10^{-6})$

$E'_{H,oxidant} = -0.34 - (-0.12) = -0.22$ V

Using Visual Minteq, we found $UO_2(CO_3)_3^{4-}$ to be the dominant U(VI) species for our experiment conditions (pH 7.0, 30 mM $NaHCO_3$). ΔG_f° are listed in Table S2.

Table S2 Gibbs free energy of formation for species used in U thermodynamic calculations. All values from Guillaumont et al. (2003) *Update on the chemical thermodynamics of uranium, neptumium, plutonium, americium, and technetium*. Elsevier B.V.: Amsterdam.

Species	ΔG_f° (kJ/mol)
$UO_{2(am)}$	-977 to -1003.6
$UO_2(CO_3)_3^{4-}$	-2660.9
HCO^{3-}	-586.8
H^+	0

$UO_2(CO_3)_3^{4-} + 3H^+ + 2e- \rightarrow UO_2(s) + 3HCO_3^-$

$\Delta G^0_r = \Delta G^0_{f\,UO2(s)} + 3*\Delta G^0_{f\,HCO3-} - \Delta G^0_{f\,UO2(CO3)3\,4-}$

if $\Delta G^0_{f\,UO2(s)}$ = -977 kJ/mol, then:

ΔG^0_r (kJ/mol) = -977 + 3*(-586.8) – (-2660.9) = -76.5 kJ/mol

$E^0_H = -\Delta G^0_r/nF$ = -(-76,500)/(2*96,485) = +0.40 V

$E^{0\prime}_H = E^0_H - 0.059/n*\log Q$

$E^{0\prime}_H$ = +0.40 - 0.059/2*log(1/((10^{-7})^3) = -0.22 V

Then plugging in values from the end of 80 d uraninite oxidation experiment:

$E'_{H,reductant} = E^0_H - 0.059/n*\log Q = +0.40 - 0.059/2*\log([HCO_3^-]^3/([UO_2(CO_3)_3^{4-}]*[H^+]^3))$

$E'_{H,reductant} = +0.40 – (0.059/2)*\log[(0.024)^3/(236*10^{-6})*(10^{-7})^3)]$

$E'_{H,reductant}$ = +0.40 – (0.059/2)*19.77 = -0.18 V

$E'_{H,overall} = E'_{H,oxidant} – E'_{H,reductant}$ = -0.22 – (-0.18) = -0.04 V

Repeat these calculations for $\Delta G^0_{f\,UO2(s)}$ = -1003.6 kJ/mol:

ΔG^0_r (kJ/mol) = -1003.6 + 3*(-586.8) – (-2660.9) = -103 kJ/mol

$E^0_H = -\Delta G^0_r/nF$ = -(-103,000)/(2*96,485) = +0.53 V

E'^0_H = +0.53 - 0.059/2*log(1/((10^{-7})^3) = -0.09 V

Similar to above:

$E'_{H,reductant}$ = +0.53 – (0.059/2)*19.77 = -0.05 V

$E'_{H,overall}$ = $E'_{H,oxidant}$ – $E'_{H,reductant}$ = -0.22 – (-0.05) = -0.17 V

Table S3 Comparison of calculated values for $E'_{H,oxidant}$ (nontronite NAu-2) and $E'_{H,reductant}$ (uraninite) from abiotic reduction experiments.

Clay-Fe(II) (μM)	Clay-Fe(III) (μM)	Fe(II)/Fe(III)	$UO_{2(am)}$ (μM)	$U(VI)_{aq}$ (μM)	$E'_{H,oxidant}$ (V) = $E'_{H,clay\text{-}Fe(II/III)}$	$-E'_{H,reductant}$ (V) = $E'_{H,U(IV/VI)}$	$E'_{H,overall}$ (V)
336	1714	0.20	169	236	-0.22	-0.18 [a]	-0.04
336	1714	0.20	169	236	-0.22	-0.05 [b]	-0.17

$E'_{H,overall}$ = $E'_{H,oxidant}$ – $E'_{H,reductant}$

[a] calculated with ΔG_f° of amorphous uraninite = -977 kJ/mol

[b] calculated with ΔG_f° of amorphous uraninite = -1,003.6 kJ/mol

Example thermodynamic calculations for abiotic AH_2DS experiments:

$0.5AQDS + H^+ + e^- \rightarrow 0.5AH_2DS$ $\quad E^0_H$ = +0.23 V

$E^{0\prime}_H = E^0_H - 0.059/n*\log Q$

$E^{0\prime}_H$ = +0.23 - 0.059/1*log(1/1*(10^{-7})) = -0.18 V

As example, plug in values from experiment with 200 μM AH_2DS and 0.25 g/L NAu-2 (Table S4)

$E'_{H,oxidant}$ = -0.34 – (1/0.36)*(0.059/1)*log(184*10^{-6}/841*10^{-6})

$E'_{H,oxidant}$ = -0.34 – (-0.11) = -0.23 V

$E'_{H,reductant}$ = +0.23 - 0.059/1*log(94*10^{-6}/(106*10^{-6}*10^{-7}))

$E'_{H,reductant}$ = +0.23 – (0.41) = -0.18 V

$E'_{H,overall}$ = $E'_{H,oxidant}$ – $E'_{H,reductant}$ = -0.23 – (-0.18) = -0.05 V

Table S4 Comparison of calculated values for $E'_{H,oxidant}$ (nontronite NAu-2) and $E'_{H,reductant}$ (AH_2DS) from abiotic reduction experiments.

Clay-Fe(II) (μM)	Clay-Fe(III) (μM)	Fe(II)/Fe(III)	AQDS (μM)	AH_2DS (μM)	$E'_{H,oxidant}$ = $E'_{H,clay\text{-}Fe(II/III)}$	$E'_{H,reductant}$ = $E'_{H,AH2DS/AQDS}$	$E'_{H,overall}$ (V)
184	841	0.22	106	94	-0.23	-0.18	-0.05
186	839	0.22	103	292	-0.23	-0.20	-0.03
192	833	0.23	105	709	-0.24	-0.21	-0.03
738	3362	0.22	376	27	-0.23	-0.15	-0.08
780	3320	0.23	413	387	-0.24	-0.18	-0.06

$E'_{H,overall} = E'_{H,oxidant} - E'_{H,reductant}$

SI-3 Bioreduction Data

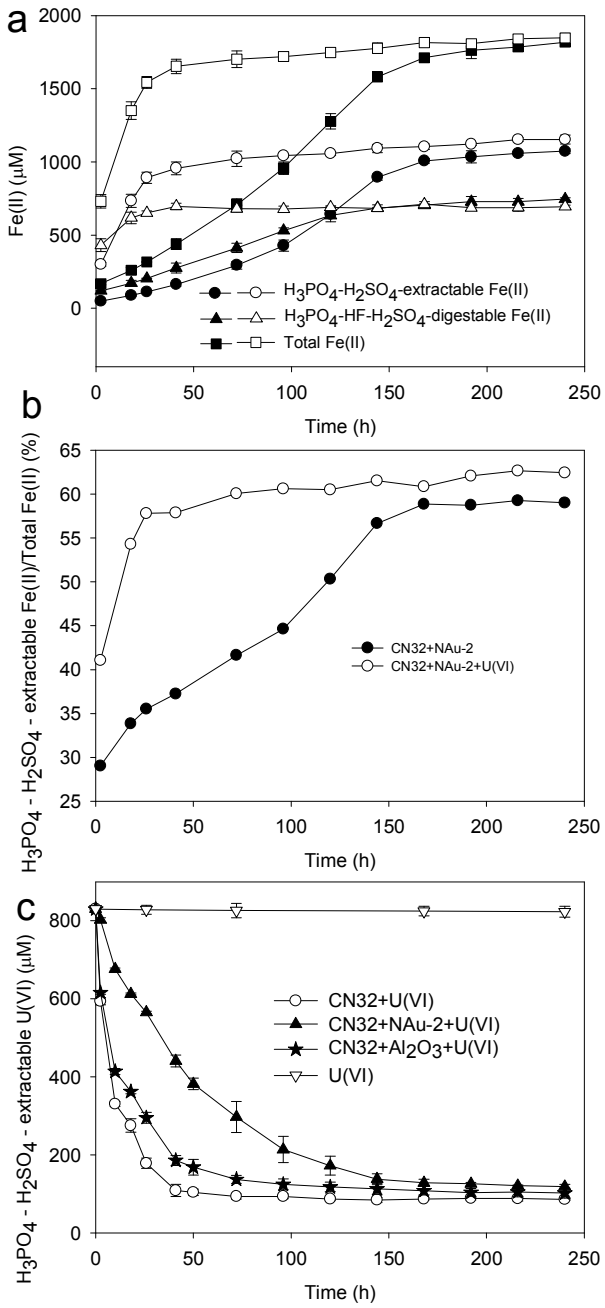

Figure S2. Bioreduction of nontronite NAu-2 and uranium (VI). Experiments conducted with $1*10^8$ cell mL^{-1} CN32, 2.0 g L^{-1} NAu-2 (or 2.0 g L^{-1} Al_2O_3) and 830 μM uranyl acetate (U(VI)) in 10 mM PIPES - 30 mM $NaHCO_3$ buffer (pH 7.0). a. Fe(II) concentrations versus time. Solid symbols are reactors containing CN32 + NAu-2 and open symbols are reactors containing CN32 + NAu-2 + U(VI). b. The ratio of H_3PO_4-H_2SO_4-extractable Fe(II) / Total Fe(II) (%) versus time. c. U(VI) concentrations versus time. Symbols represent means of triplicate measurements and error bars represent 1 standard deviation.

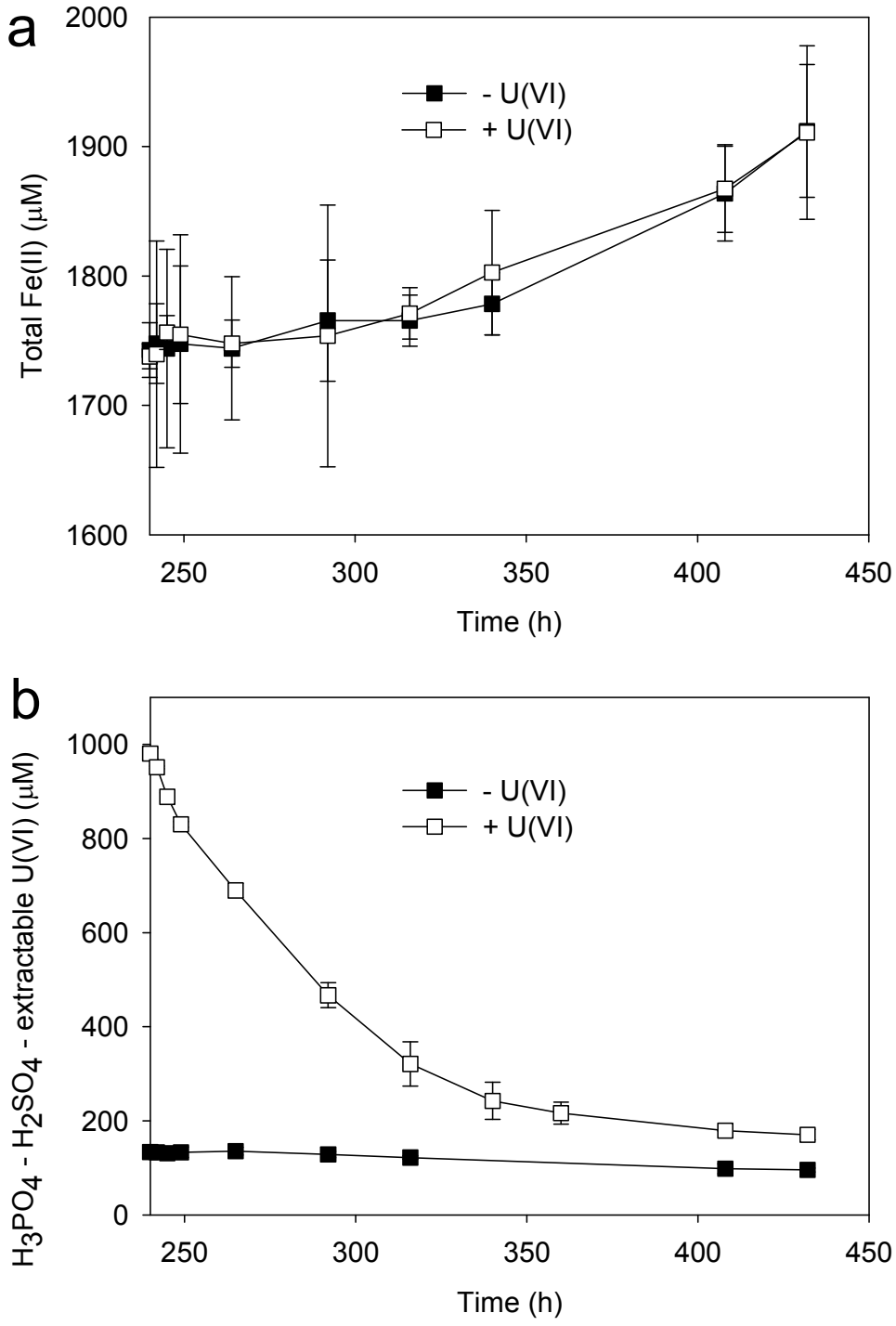

Figure S3. Bioreduction of "pre-bioreduced" nontronite NAu-2 and uranium (VI). a. Fe(II) concentrations versus time. Total Fe(II) = H_3PO_4-H_2SO_4-extractable Fe(II) + HF-H_2SO_4-digestable Fe(II). b. U(VI) concentrations versus time. 850 μM uranyl acetate and 5 mM sodium lactate were added into the reactors after 240 h.

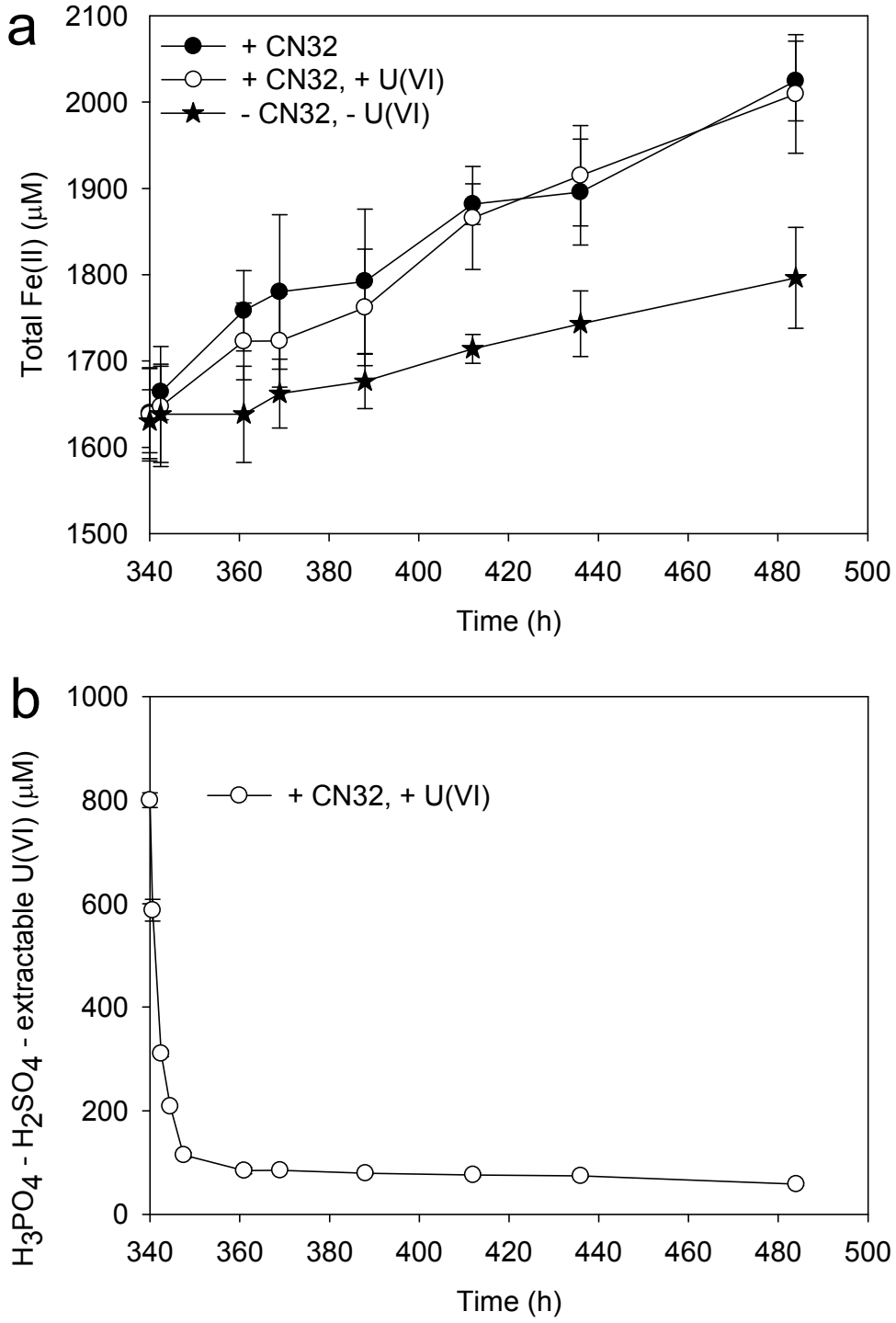

Figure S4. Bioreduction of "pre-bioreduced" nontronite NAu-2 and uranium (VI). a. Fe(II) concentrations versus time. Total Fe(II) = H_3PO_4-H_2SO_4-extractable Fe(II) + HF-H_2SO_4-digestable Fe(II). b. U(VI) concentrations versus time. $1*10^8$ cell mL^{-1} CN32, 800 μM uranyl acetate and 5 mM sodium lactate were added into the reactors after 340 h.

SI-4 Abiotic Reduction Data

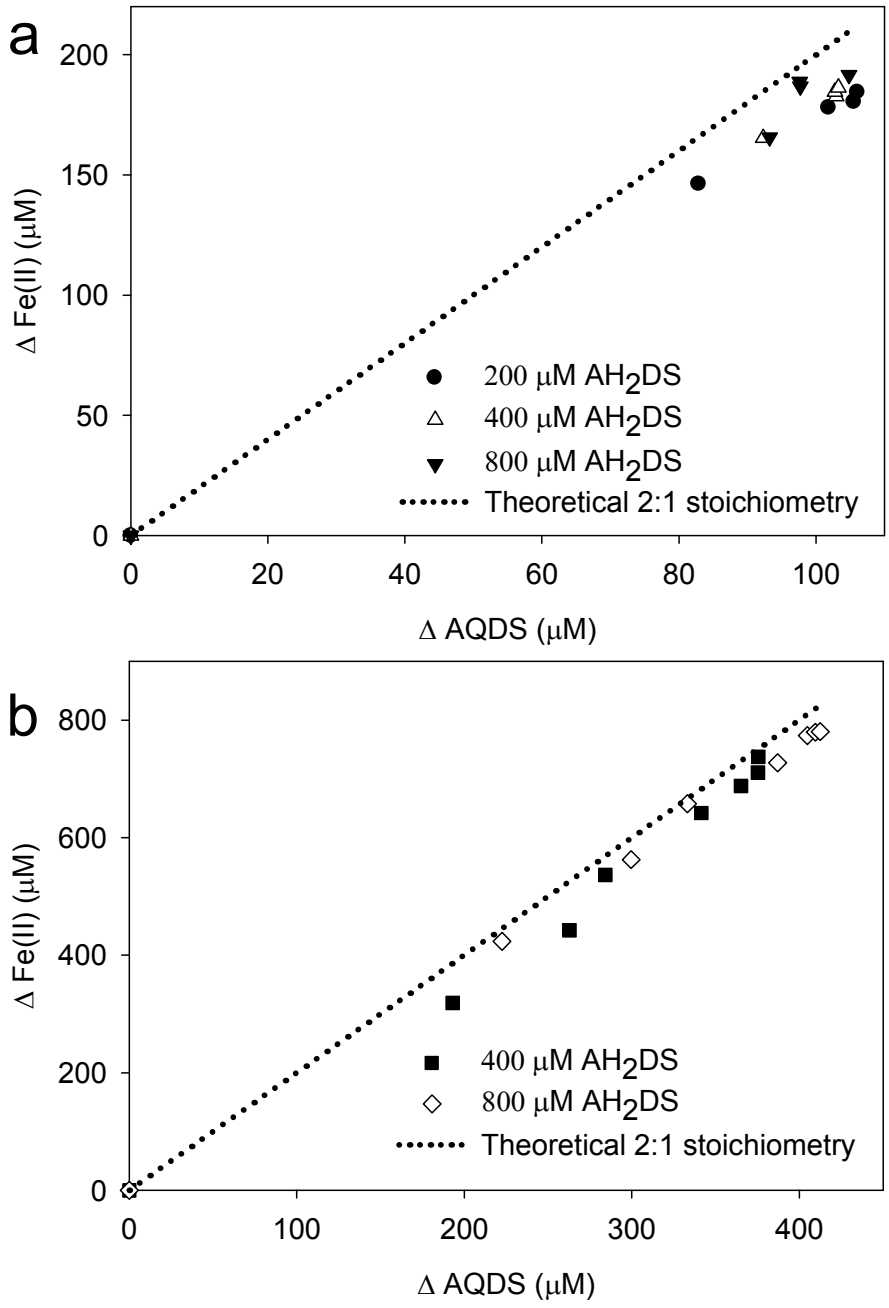

Figure S5. Stoichiometric relationship between Δ mol Fe(II) and Δ mol AQDS. a. Experiments conducted with 0.25 g L^{-1} NAu-2 and 200 to 800 μM AH_2DS. b. Experiments conducted with 1.0 g L^{-1} NAu-2 and 400 to 800 μM AH_2DS. Dashed line represents theoretical stoichiometry of 2 mol Fe(II) to 1 mol AQDS.

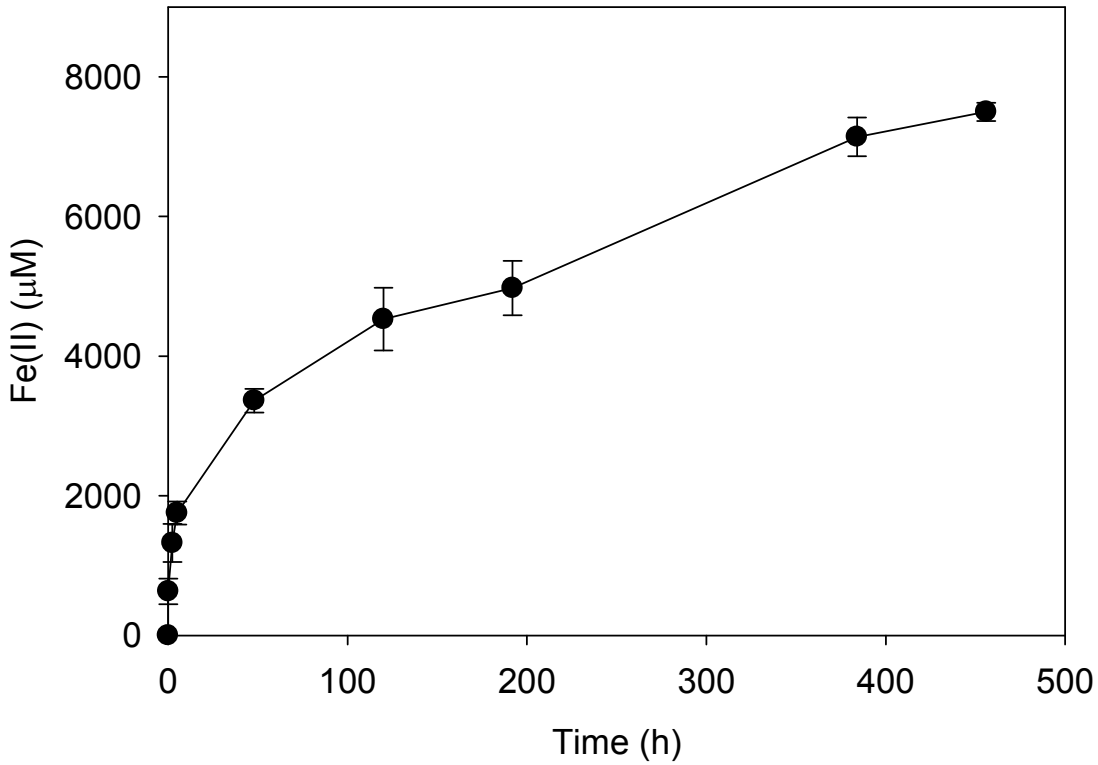

Figure S6. Abiotic reduction of nontronite NAu-2 by sodium dithionite. Experiments conducted with 2.0 g L^{-1} Nontronite and 6 g L^{-1} sodium dithionite in sodium citrate (266 mM) - sodium bicarbonate (111 mM) buffer at room temperature